Chapter 4

# Chemical Kinetic and High Fidelity Modeling of Transesterification

Isam Janajreh and Manar Almazrouei

Additional information is available at the end of the chapter

http://dx.doi.org/10.5772/intechopen.80008

**Abstract**

The modeling and simulation of transesterification require an understanding of the chemical reactions that take place inside the reactor. The development of reaction mechanism of the multiple step triglyceride, triglycerides and mono-glycerides and their reversal reaction is beyond the interest of chemical or mechanical engineers, whose main interests are to assess the conversion overall and to establish performance process metrics. This chapter undertakes the transesterification conversion by firstly establishing and formulating the overall process kinetics as far as the rate constant and activation energy. Secondly, use the obtained kinetic values to carry out high fidelity reactive flow of the multiple species which are co-present inside the reactor and otherwise complex to capture experimentally. Following these two steps, this work provides qualitative and quantitative information on the concentration of the reactants, intermediates and the overall yield. This two-step-approach can also be utilized as reactor design tool and gaining in-depth insight on reaction progress and species distribution. Experimental results, high-fidelity numerical results, and parametric sensitivity studies will be introduced and discussed.

**Keywords:** chemical kinetic, transesterification, CFD, biodiesel, crude glycerol

## 1. Introduction

Stoichiometrically and theoretically speaking, transesterification consumes 1 mole of triglyceride and 3 moles of alcohol to produce 3 moles of fatty acid methyl esters (FAME) and 1 mole of crude glycerol. Practically, unconverted triglyceride (TG) and intermediates (i.e. diglyceride (DG) and monoglyceride (MG)) co-present in the yield which signifies the incompletion of the reaction [1]. As these reactions are mildly influenced by temperature and pressure because of their nearly equal heat of formation and liquid phase, the increase in the molarity of the alcohol

| Species | Chemical formula | Molecular weight (g/mol) | Viscosity (kg/m.s) | $C_p$ (J/kg.°C) | Density (kg/m$^3$) |
|---|---|---|---|---|---|
| Methanol | $CH_4O$ | 32 | 3.96E-4 | 1.470E3 | 791.8 |
| Waste oil or Triglyceride | $C_{54}H_{105}O_6$ | 848 | 1.61E-2 | 2.2E3 | 883.3 |
| Diglyceride | $C_{37}H_{72}O_5$ | 596 | — | — | 880 |
| Monoglyceride | $C_{20}H_{40}O_4$ | 344 | — | — | 875 |
| Biodiesel | $C_{18}H_{36}O_6$ | 284 | 1.12E-3 | 1.187E3 | 870 |
| Glycerol | $C_3H_9O_3$ | 93 | 1.412E0 | 0238.6 | 1261 |

**Table 1.** Summary of species properties and molecular weight (MW) [5].

promotes the desired forward reaction [2]. Contrary to well-known hydrocarbon fuels that are characterized by fixed thermodynamic and physical properties, the TG, DG, MG have no fixed chemical formula and neither their thermodynamic properties, such as standard enthalpy or specific heats, nor physical ones like density or viscosity, are consistent throughout the literature [3, 4]. Therefore, material characterization is an essential step in the modeling of the transesterification process. The extent of these properties depends on the complexity and comprehensiveness of the simulation, from a simple incompressible flow that requires only viscosity and density, to a complex non-isothermal flow that requires heat of formation, specific heat, thermal conductivity and their associated diffusions. However, as these properties can be derived following the American Society for Testing and Materials (ASTM) standards, their reactions are more complex. **Table 1** summarizes some of the utilized properties for the waste oil, TG, DG, and MG used in the work of Noureddine and Zhu who were amongst the pioneers of quantifying transesterification reaction kinetics [5].

Setting up a reaction mechanism of numerous species or elements and hundreds of reactions, while accounting for reaction radicals, is rather impractical for engineers. The overall reaction can be captured through well controlled conditions and yield assessment procedures that can save the pain of the development or use these reaction mechanisms. This chapter undertakes the conventional transesterification at different process temperatures, highlighting their influence on the yield and their distribution inside the reactor.

## 2. Biodiesel feedstock and the reactor device

While corn, sunflower, and palm oil are readily available in the market, their utilization may raise a strong debate on land for food vs. land for energy. To rule out this debate, waste cooking oil (WCO) is used instead, because it is abundantly available feedstock, inexpensive and most of the time its disposal into sewerage systems is associated with environmental concerns. The supply chain of collecting this abundant source is beyond the scope of this

chapter. However, it is important to state that residential communities are in general in favor of trapping this problematic sewerage source that is responsible for clogging the plumbing systems. Collection also can be facilitated by using drum type or smaller plastic containers provided to the local restaurant, school/university canteens, residential communities as a privately owned small business, or through municipality.

The collected WCO generally requires pretreatment that can be facilitated at a moderate temperature to maintain its liquid and less viscous form. One can use the heat of the summer (45–50°C) at which unsaturated and saturated steric fatty acid stays in liquid form, and 10–20 μm filtration can be used to eliminate any suspended oil solid residuals. Dehydrating of the WCO is also required, during which any water content brought by the processed food into the waste cooking oil is liberated through evaporation. At the laboratory scale, stirring and heating pad at near 110°C for several hours can perfect this task. Process methanol and catalyst NaOH or KOH can also be substituted with commercially available grade instead of high purity pharmaceutical grade/Sigma-Aldrich that can also leverage process economically. Once pretreatment of the feedstock is done, the NaOH solid catalyst in the form of small ballets is dissolved into methanol at the stipulated ratio, i.e. 0.5–1% by mass of WCO. This process can be facilitated under moderate heating and a temperature below 60°C and stirring forming the meth oxide reactant solution. In the lab, multiple transesterification reaction experiments can be conducted simultaneously under the same temperature and stirring rate to reduce experimental sequence and human error. This can be carried out using a multiple dissolution apparatus such as those provided by *Agilent Technologies*, featuring 6–12 reactor vessels as depicted in **Figure 1** [6]. The caps are tightly fitted and are equipped with direct access ports for sampling without process interruption. They all are also set on thermally controlled wells. The process in these individual small-scale batch reactors resemble those carried out in larger

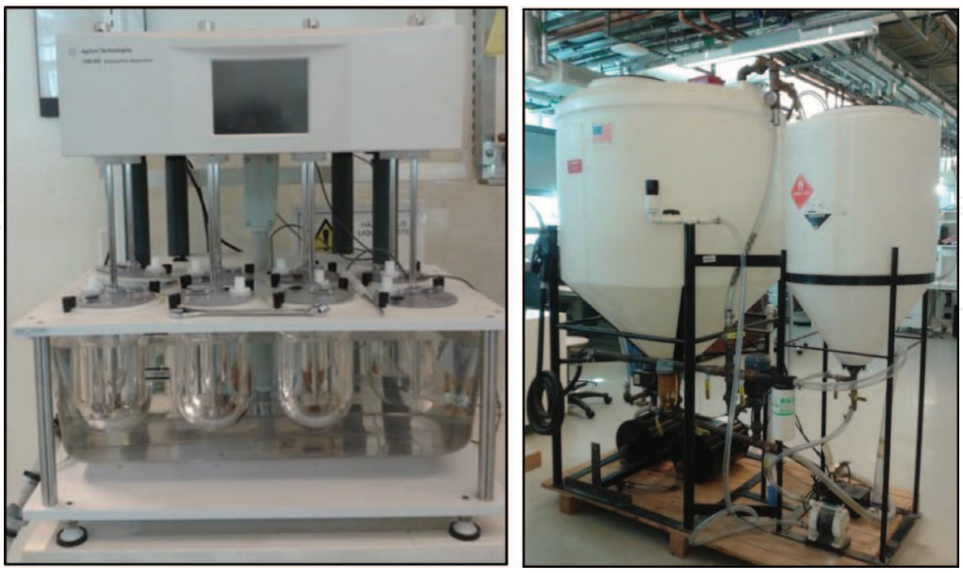

**Figure 1.** Dissolution apparatus representing eight multiple 1-L batch reactors and *HomeBiodeselKits* 500-liter batch reactor.

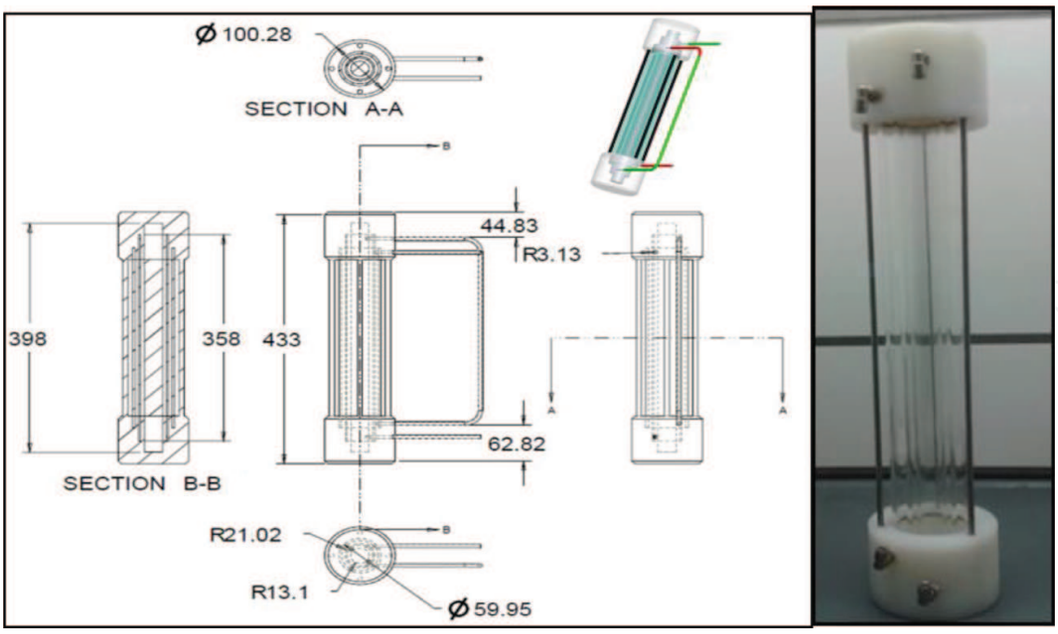


**Figure 2.** Patented tubular continuous biodiesel reactor 1–8L/hr [19].

scale ones provided by *HomeBiodeselKits*, as depicted in **Figure 1**. Beside batch method, a patented continuous reactor is also depicted in **Figure 2** featuring compactness, continuity, and scalability. This reactor reported better efficacy observed by the higher throughput and better quality of product than the batch reactor.

The continuous reactor consists of a tubular reactor of two or more upright concentric cylinders. Each is equipped with inflow at the bottom and outflow at the top port, connected by 5-mm ϕ chemically resistive hoses. The inflow and outflow are configured circumferentially in each cylinder, rendering the flow more residence time due to their helical trajectory. The details of the reactor's dimensions and geometry can be found in the work of Janajreh et al. [7]. A peristaltic or a diaphragm pump type is used to inject the two reactants, i.e. pretreated oil and methoxide into the reactor at the stipulated molar ratio. The mass flow rate is typically being set beyond laminar limits for turbulence mixing that help the transesterification reaction. The mixture from the batch dissolution is periodically recovered in 10 mm vials, and is refrigerated to halt their progressive reactions for downstream species analysis. The analysis of the compositions of TG, DG, MG, FAME, glycerol (GL) and alcohol (AL) is carried out using a standard Gas Chromatography Mass Spectrometry (GC/MS) equipment as those provided by *Thermo Scientific DSQ II* equipped with a flame ionization detector.

In the GC/MS analytical equipment, the FAME column is initially calibrated using standard biodiesel and glycerol samples to ensure precise qualitative and quantitative analysis. The collected and refrigerated vials are obtained at numerous and progressive reaction intervals of 15-time steps over 2 hr of reaction time [8]. The breakdown of sample species composition is acquired using methods similar to those carried out by Noureddini and Zhu [5] and Janajreh et al. [7]. Transesterification is performed at 6:1 alcohol to oil molar ratio and 0.5% NaOH by mass of WCO, and both at different temperatures of 50 and 60°C.

http://dx.doi.org/10.5772/intechopen.80008

## 3. Transesterification method

**Figure 3** shows the three-step details of the three equilibrium reactions process of transesterification reaction as indicated by Noureddine et al. [5] and Janajreh et al. [9].

This equilibrium given in **Figure 1** is represented by six coupled first order differential equations including the overall shunt reaction as per Eqs. (1)–(6) [10] and these are written as:

$$d[TG]/dt = -k_1[TG][AL] + k_2[E][DG] - k_7[TG][AL]^3 + k_8[E]^3[GL] \quad (1)$$

$$d[DG]/dt = -k_3[DG][AL] + k_4[E][MG] + k_1[TG][AL] - k_2[E][DG] \quad (2)$$

$$d[MG]/dt = -k_5[MG][AL] + k_6[E][GL] + k_3[DG][AL] - k_4[E][MG] \quad (3)$$

$$d[E]/dt = k_1[TG][AL] - k_2[E][DG] + k_3[DG][AL] - k_4[E][MG] + k_5[MG][AL] - k_6[E][GL] + k_7[TG][AL]^3 - k_8[E]^3[GL] \quad (4)$$

$$d[GL]/dt = k_5[MG][AL] - k_6[E][GL] + k_7[TG][AL]^3 - k_8[E]^3[GL] \quad (5)$$

$$d[AL]/dt = -d[E]/dt \quad (6)$$

In these equations, $k$ is the rate constant of each of the forward and backward reaction of **Figure 3** and $(x)$ is the concentration of species $x$, the $TG$, $DG$, $MG$, $AL$, $E$, and $GL$ are

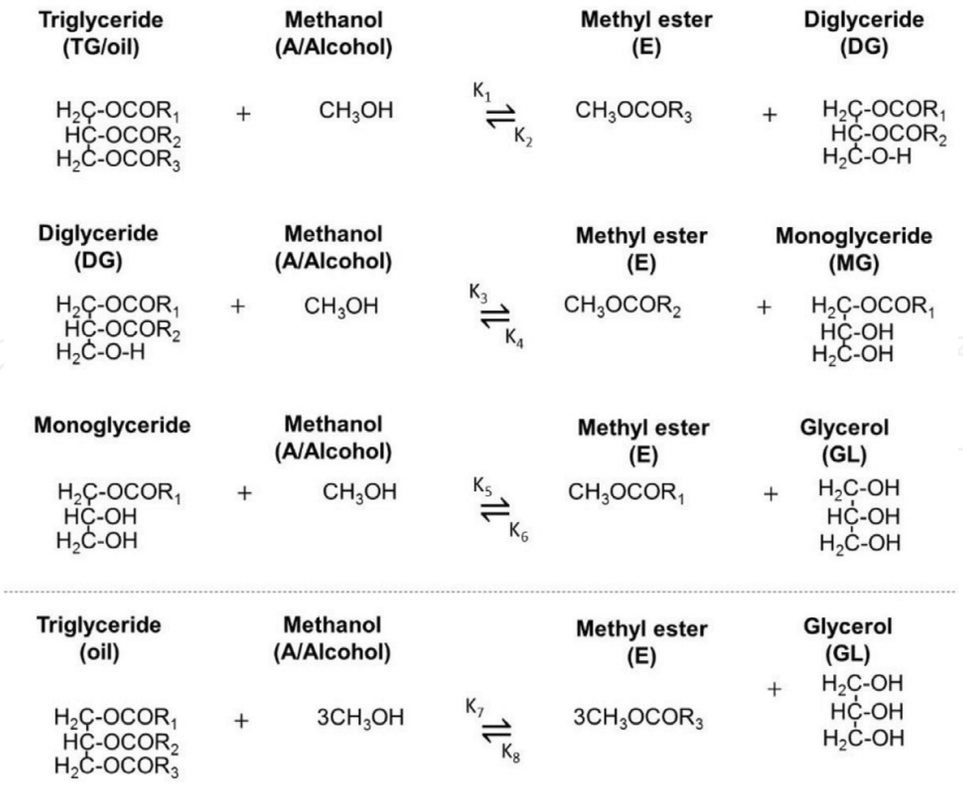


**Figure 3.** Transesterification reaction mechanism.

respectively the Triglyceride, Diglyceride, Monoglyceride, Alcohol, Fatty Acid Methyl Ester and Glycerol. This system of PDEs Eqs. (1)–(6) is solved for $k_1$ through $k_8$ at minimum root mean square following the temporal measurements of each specie and using Eq. (7) as:

$$Ax = b \; or \; x = A^{-1}b \tag{7}$$

where $A$ is the coefficient matrix of the species concentration at each time step obtained through GC/MS analysis, $x$ is the evaluated rate constant vector ($k_1$ through $k_8$) and $b$ is obtained by evaluating the time derivative of the measured concentrations. The rate constant ($k$) of each reaction is expressed by the Arrhenius Eq. (8) [11] as follows:

$$k = A_o e^{-E/RT} \text{ or } \ln k = \ln A_o - \frac{E}{R}\frac{1}{T} \tag{8}$$

where $A_o$ ($s^{-1}$) is the pre-exponential constant, $E$ (J/mol) is the activation energy corresponding to each of the eight reactions, $R$ (J/mol K) is the molar universal gas constant and $T$ is the process temperature expressed in degree Kelvin. Therefore, from the slope and intercept of the natural log line of $K$ and $1/T$ one can infer the activation energy (which is normalized by the gas constant) and the natural log of the pre-constant, respectively. Following previous work on chemical kinetics [5, 12], the reaction rate constants Eqs. (1)–(8) are solved simultaneously using MATLAB which enables direct inference of $E$ and $A_o$ [13].

## 4. Transesterification kinetics evaluation

Transesterification is a slowly reversible reaction, where only the forward reactions are desired for the production of biodiesel. It is easy to say that lower activation energies are favored for forward reactions ($E1$, $E3$, $E5$, $E7$) while higher activation energies are preferred for backward reactions ($E2$, $E4$, $E6$, $E8$). Unfortunately, this is not as simple as will be stated below. The obtained GC/MS results for this conventional transesterification at 0.5% NaOH, 6:1 molar ratio and temperature of 50 and 60°C, in terms of mole fraction, are depicted in **Figure 4**. It shows the rates of consumption of TG and Alcohol into the formation of methylesters ($E$) and $GL$ as well as the intermediate species, i.e. $DG$ and $MG$.

The $E$ production and its byproduct $GL$ demonstrate a sigmoidal trend: a slow delay in the reaction rate at the start is then followed by a quick surge in the production, and a final slow rate near the reaction completion. This trend characterizes the changing mechanisms reaction that swings from the slow mass transfer controlled to the fast kinetically controlled and back to slow reactivity as equilibrium is attained [5]. This can be explained by the poor diffusion between the two phase reactants system, i.e. $TG$ and $AL$. As soon as the methyl ester is formed the solubility of the two phases into one single phase is increased drastically which causes the production surge. This is stipulated by any sample taken at the first minute of the reaction, which tends to form two separate phases. Samples taken thereafter appear to be a more homogenized single phase as sampling time progress. At the onset of the formation of the single phase, mixing becomes less important and hence temperature can play more important

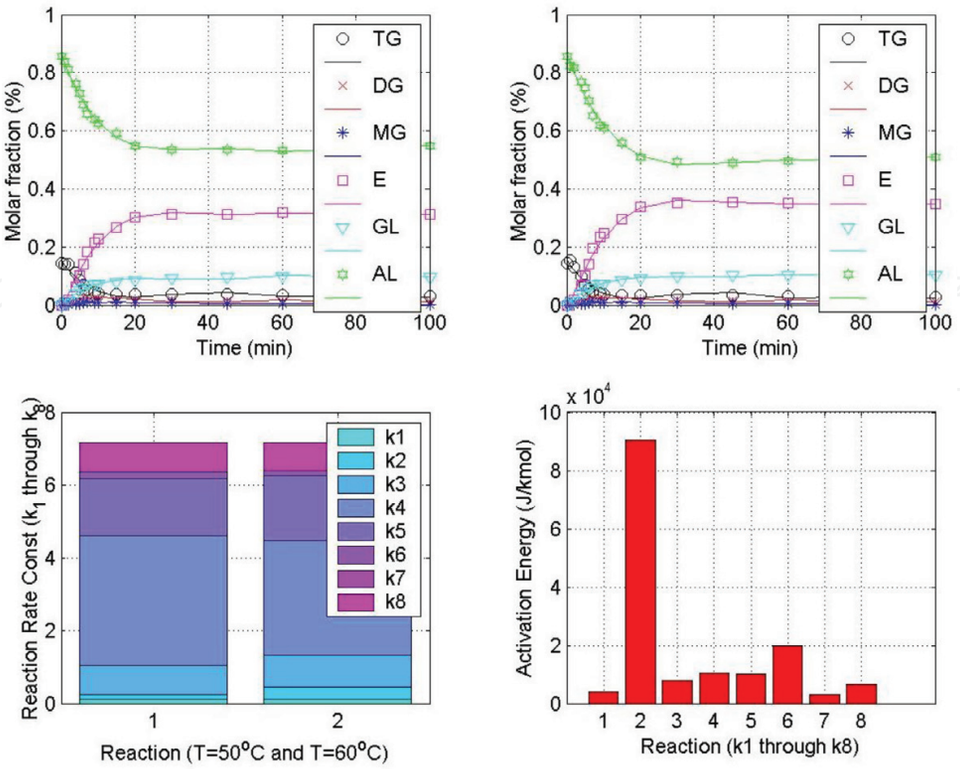


**Figure 4.** Transesterification of WCO conversion results at 50°C (top left) and 60°C (top right). Corresponding chemical kinetic reaction rate constants (bottom left) and activation energy (bottom right).

role to kinetically propel these reactions. In general, an increase in temperature provides a higher energy state for the molecules leading to more collisions and also improves the solubility of the reactants. As these reactions are reversible, the consumption of any of the reactants must be avoided to steer and ensure these reactions of **Figure 3** forward.

As can be shown in **Figure 4** of the GC/MS results obtained at the two temperatures, *DG* and *MG* are intermediate species. They appear following mass transfer limitation for a relatively shorter time, before they asymptotically vanish. The amount of unreacted alcohol at T = 60°C is shown to be lower than those obtained at T = 50°C, as per **Figure 4**. On the contrary, the *FAME* production and its byproduct *GL* is noticeably higher at higher temperature (T = 60°C) than the lower process temperature (T = 50°C). The rate constants for the two process temperatures are depicted side by side in the bottom left 'staked bar plot' of **Figure 4**. These values are relatively comparable, except for $k_2$ and $k_4$. Considering the lower temperature stacked bar (left side), it shows the low value of $k_1$ and $k_2$ reaction constants compared to the rest of reaction constants placing them as the rate limiting reactions. As soon as the product of these reactions becomes available, higher rates for their intermediate yield takeover. Comparing the lower and higher temperature $k_s$, the higher temperature results in higher $k_1$ and $k_2$, which are the rate limiting reactions, while the rest are comparable. This explains the higher initial yield beyond the two-phase mass transfer limitation that lasts within the first minutes of the reaction. These evaluated activation energies are also depicted in the bar plot of **Figure 4** on the bottom right. These

| Designated K or E | Rate constant at T = 50°C | Rate constant at T = 60°C | Activation energy (J/mol) | Pre-constant ($sec^{-1}$) |
|---|---|---|---|---|
| TG + AL—E + DG | 0.1213 | 0.1157 | 4103 | 77,983,755.8 |
| E + DG—TG + AL | 0.1167 | 0.3276 | 90,540 | 449,020.085 |
| DG + AL—E + MG | 0.8177 | 0.8947 | 7896 | 1.0976 E12 |
| E + MG—DG + AL | 3.5379 | 3.1354 | 10,597 | 4570,1701.3 |
| MG + AL—E + GL | 1.5943 | 1.7922 | 10,267 | 767.86 |
| GL + E—MG + AL | 0.1661 | 0.1322 | 19,980 | 32,870.58 |
| TG + 3AL—3E + GL | 0.001 | 0.001 | 3089 | 77,983,755.8 |
| GL + 3E—TG + 3A | 0.8149 | 0.7568 | 6490 | 449,020.085 |

**Table 2.** Summary of the rate constants values of the reactions at two temperatures and their activation energy.

are consistent with those reported experimentally by Feedman and coworkers [14, 15]. Based on the Arrhenius equations, they reported activation energies in the transesterification of the soybean oil in the range of 33,472–83,400 J/mol [16, 17]. These values are tabulated in **Table 2**, along with the rate constant. The activation energy is the highest for the reverse of the first reaction, DG + E—TG + AL suggesting this reaction is not as spontaneous as the others and reverse formation of TG is rather less expected. This is due to surplus of the Methanol alcohol that forces the forward reactivity of the TG + AL—DG + E reaction. This is also evident from all the forward reactions which are at lower activation energy than their associated reversal reaction.

The evaluated kinetics will be utilized in the development of a high fidelity reaction model. The model will be based on reactive flow of the six species, TG, AL, DG, MG, E and GL and their eight reactions. These are types of volume homogenous reactions. The considered reactor will be a tube type subjected to appropriate conditions and enabling the assessment of the yield and species distribution.

In summary, the required kinetics that governs the reactions and change of species has been evaluated. Results are intuitively correct, as a higher temperature results in higher rate constants. These data will be used in the high fidelity reactive flow analysis that will be detailed next. It is important to emphasize that importance of these simulations in capturing the overall species and their distribution in the reaction device. This is becoming the tool for the development of the new and innovative reactors. The observations procured from performing the chemical kinetic study enables the shift in conventional transesterification towards a modified sonication kinetic data for further reactive flow analysis. Comparison between regular mixing and ultra- sound assisted procedures proves the supremacy of the latter in terms of fastening the forward reactions by increasing reaction rates and decreasing activation energies of forward reactions. Note that the comparative study is performed to obtain an idea of the trend of sonication and not to get exact chemical kinetics.

http://dx.doi.org/10.5772/intechopen.80008

## 5. High-fidelity transesterification model development

In order to sharpen our understanding of the transesterification reaction progression and species distribution, a high fidelity reactive flow model for transesterification is developed. The basis of the model is computational fluid dynamics (CFD). Several research software have adopted CFD environment to solve multiple physics, whereby some are open sources and others are more commercially tuned. The transesterification model is developed within the finite volume CFD based software of Ansys/Fluent 17.1 [18].

### 5.1. Governing equations

We here focus on the modeling of the tubular reactor that depicted earlier in **Figure 2** which has numerous advantages over the batch reactor, i.e. continuous, compactness, better yield [19]. Modeling involves the application of flow continuity, momentum, and energy equations. Furthermore, the flow is characterized as a mixture of multiple reacting species, incompressible, viscous, and turbulent. The reaction is assumed to start as soon as the reactant components are met inside the reactor. The flow is governed by the Navier-Stokes equation, which is associated with temporal, advective, viscous, and any source term and is written as:

$$\frac{\partial}{\partial t}(\varnothing) + \frac{\partial}{\partial x_i}(u_i \varnothing) = \frac{-\partial}{\partial x_i}\left(\Gamma_\varnothing \frac{\partial \varnothing}{\partial x_i}\right) + S_\varnothing \tag{9}$$

where $u_i$ is the velocity and $S_\varnothing$ is the source term due to the dispersed phase interaction. The $\varnothing$ is the flow dependent variable and when represents the density ($\rho$), velocity density multiple ($\rho u_i$) and the temperature ($T$) it yields the continuity, the momentum, and the energy equations, respectively. It takes also the turbulent scalars, i.e. kinetic energy ($k$) and dissipation rate ($\varepsilon$). These two equations in steady state are expressed as:

$$\begin{aligned} \rho u_i \frac{\partial k}{\partial x_i} &= \mu_t \left(\frac{\partial u_j}{\partial x_i} + \frac{\partial u_i}{\partial x_j}\right)\frac{\partial u_j}{\partial x_i} + - \frac{\partial}{\partial x_i}\left(\frac{\mu_t}{\sigma_k}\frac{\partial k}{\partial x_i}\right) - \rho\varepsilon \\ \rho u_i \frac{\partial \varepsilon}{\partial x_i} &= C_{1\varepsilon}\frac{\mu_t \varepsilon}{k}\left(\frac{\partial u_j}{\partial x_i} + \frac{\partial u_i}{\partial x_j}\right)\frac{\partial u_j}{\partial x_i} + \frac{\partial}{\partial x_i}\left(\frac{\mu_t}{\sigma_\varepsilon}\frac{\partial \varepsilon}{\partial x_i}\right) - C_{2\varepsilon}\frac{\rho\varepsilon^2}{k} \end{aligned} \tag{10}$$

The left terms govern the advective while the right hand terms govern respectively the generation, the diffusion, and destruction of the turbulent quantities. In these equations, $\mu_t$ is the eddy viscosity parameter and it overwhelms the laminar viscosity and is written as:

$$\mu_t = f_\mu C_\mu \rho k^2 / \varepsilon \tag{11}$$

where $f_\mu$ and $C_\mu$ are flow dependent constants and $C_{1\varepsilon}$, $C_{2\varepsilon}$,$\sigma_k$ and $\sigma_s$ are tuning empirical constants. The transport equations that govern the of species $m_i$ take the following form:

$$\frac{\partial}{\partial t}(\rho m_i) + \frac{\partial}{\partial x_j}(\rho u_j m_i) = \frac{\partial}{\partial x_j}(\rho D_{i,m} + \mu_t / Sc_t)\frac{\partial m_i}{\partial x_j} + R_i + S_i \tag{12}$$

Here $D_{i,m}$ is the diffusion coefficient of $i$ specie within the $m$ bulk species and $Sc_t$ is the turbulent Schmidt number defined as the ratio of the eddy viscosity t to the eddy diffusivity $D_{i,m}$. Eq. 10 incorporate an additional source term $R_i$ which accounts for species reaction. This term is governed by the reaction stoichiometry of the specie $m_i$ and is written as:

$$\sum_{i=1}^{N} v'_{i,r} S_i \underset{k_{b,r}}{\overset{k_{f,r}}{\Leftrightarrow}} \sum_{i=1}^{N} v''_{i,r} S_i \tag{13}$$

The reaction rate is proportional to the concentration of the reaction species (both reactants and products) to an ordered of specified power coefficients that can be written as:

$$R_{i,r} = M_{i,r}(v''_{i,r} - v'_{i,r})\left(k_f \prod_{j=1}^{N} C_{j,r}^{\eta^*_{,rj}} - k_b \prod_{j=1}^{N} C_{j,r}^{v'^*_{j,r}}\right) \tag{14}$$

where $k_f$ ($k_1$, $k_3$, $k_5$, $k_7$) and $k_b$ ($k_2$, $k_4$, $k_6$, $k_8$) are the reaction rate constants evaluated according to Eq. (8) for the forward and backward of the above Arrhenius equation Eq. (13) that summarizes equations of **Figure 3**. The $Cj$ are the molar concentration of jth specie to the order of its stoichiometric coefficient $v$ while $\eta$ is the reaction order. The $M_i$ is the molecular weight of species i [20]. It is a good practice to pursue CFD as a non-reactive flow first before accounting the influence of reactions that numerically may induce earlier instability for the solution. After achieving near steady and consistent solution and influence of reaction can be included and analyzed.

### 5.2. CFD setup and mesh sensitivity analysis

The model of the considered tubular reactor is shown below in **Figure 5** along with its dimensions as summarized in **Table 3**.

A hybrid mesh of hexagonal and pyramid type is used to maintain the size within the processing capacity of the current laptop for an engineer. The mesh is established in *ANSYS Design Modeler,* consisting of two concentric tubular chambers along with the connecting tubing as shown in **Figure 6**. A baseline and another two refined meshes were created to study the dependency and the goodness of the mesh influence on the solution. The properties of the reactants and products are summarized in **Table 4** as per the work of Narvaez et al. [21]. The ideal mixture is used to determine the mixture properties from the known properties of the individual specie as per Eq. (15).

$$\varphi_m = \sum_{i=1}^{n} m_{f,i} \varphi_i \tag{15}$$

The boundary conditions are assigned as flow, constant velocity at the inlet and isothermal fluid. The boundary at the top outlet was defined as fixed pressure outlet at 0-Pa gauge pressure while the boundary walls are subjected to zero velocity, i.e. no slip and no penetration. The turbulence is accounted for via standard $k$-$\varepsilon$ mode and model constants were kept at their common values [22–24]. The setup was initialized at the same values of velocity from the

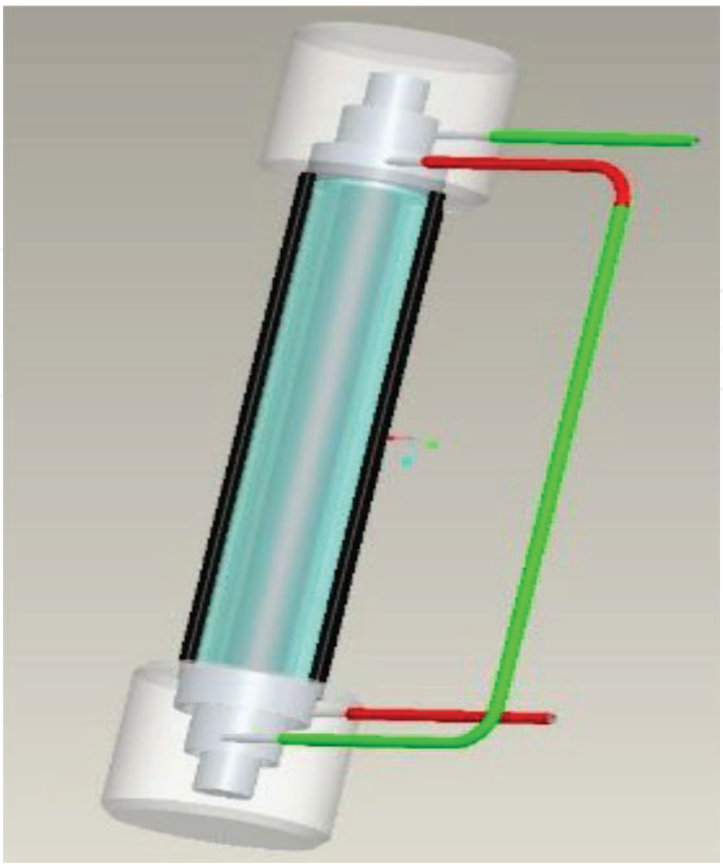

**Figure 5.** Tubular reactor model.

| Component | Outer cylinder (glass) | Middle cylinder (metal) | Inner cylinder (metal) |
|---|---|---|---|
| Outer diameter (mm) | 59.9 | 42.0 | 26.2 |
| Inner diameter (mm) | 51.9 | 36.7 | 21.8 |
| Thickness (mm) | 4.0 | 2.7 | 2.2 |
| Length (mm) | 272 | 313 | 353 |

**Table 3.** Dimensions of the reactor geometry components.

inlet boundary condition. The material initially is assumed as an ideal mixture that has the viscosity and density property proportion of 6:1 methanol-to-waste cooking oil mole fraction.

Results of the unreacted isothermal flow distribution within the reactor, or cold flow as referred to in some literature, is depicted in **Figure 7**. Velocity vector colored by the residence time is used for the three level meshes. Results of residence time parameter is used as the most pronounced parameter for the intended reactive fluid to assess the mesh accuracy. These results are summarized in **Table 5** for the three levels of the mesh for comparison. The baseline residence time is within 2% deviation from the next refined mesh, hence it is used for the rest of the analysis. However, the coarse mesh showed a sustainable deviation of nearly 10% that fails to be qualified as an accurate and representative mesh.

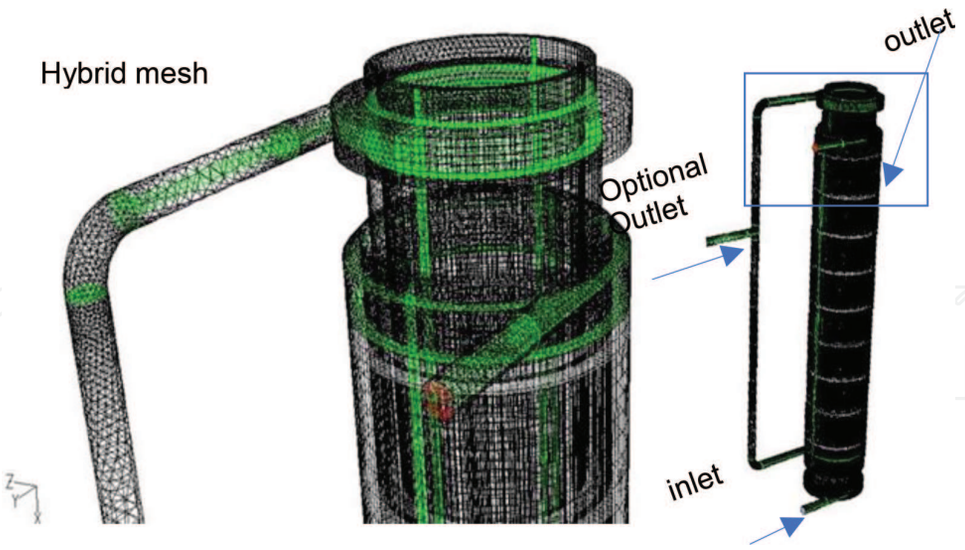


**Figure 6.** Discretized reactor domain using hybrid 3-D baseline mesh.

| Species | Chemical formula | Molecular weight (g/mol) | Viscosity (kg/m.s) | Cp (J/kg.°C) | Density (kg/m$^3$) |
|---|---|---|---|---|---|
| Methanol | $CH_4O$ | 32 | 3.96e-4 | 1.470e3 | 791.8 |
| Waste oil | $C_{54}H_{104}O_6$ | 849 | 1.61e-2 | 2.2e3 | 883.3 |
| Biodiesel | $C_{18}H_{36}O_2$ | 284 | 1.12e-3 | 1.187e3 | 870 |
| Glycerol | $C_3H_8O_3$ | 92 | 1.412e0 | 0238.6 | 1261 |

**Table 4.** Properties of the flow species.

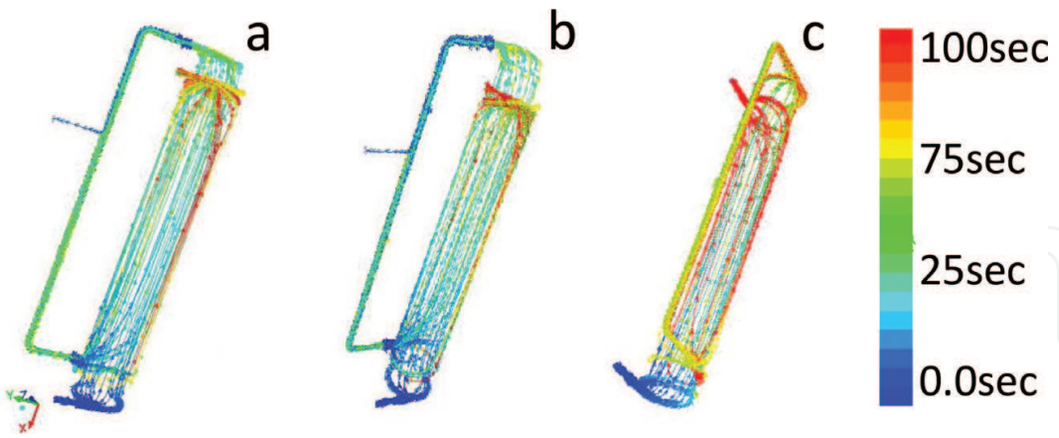


**Figure 7.** Flow trajectory colored by the resident time for the (a) baseline, (b) fine and (c) very fine.

A total resident time of the order of $10^3$ seconds is observed in each of the three meshes. If the flow was injected at relatively high velocity, it would ensure the required homogenize mixing of the reactants that also avoid any of the mass transfer limitation. The circumferential configuration of the entry and exit of the reactor enables it to maintain a long residence time, even at a higher inlet mass flow that forces the flow to move in a swirling trajectory.

| Mesh type | Coarse | Baseline (Baseline × 1.5) | Fine mesh (Baseline × 1.89) |
|---|---|---|---|
| No. of cells | 281,382 | 427,742 | 534,228 |
| Residence time (sec) | $1.01 \times 10^3$ | $1.080 \times 10^3$ | $1.100 \times 10^3$ |
| Error % | 10% | 2% | — |

**Table 5.** Cells for the two meshes for the mesh sensitivity analysis.

### 5.3. Reactive flow analysis

The reactor tube is setup vertically and is subjected to inlet flow rate at Re = 6000 at the bottom of the tube into the inner reactor chamber. There, the two fluids of TG and methoxide (mixture of the methanol and the catalyst) are injected circumferentially at the stipulated molar/mass ratio and inlet temperature. The outflow is subjected to atmospheric pressure which is admitted at exit boundary condition of the outer tube chamber located at the top. The no-lip no penetration and insulated wall is also applied to all the bounded reactor walls.

To maintain single-phase flow avoiding the complication of other reactivation, the case of reactive flow simulation is carried out below the boiling point of methanol at a temperature of 60°C (333 K). A steady-state solution is sought for the flow. This is achieved by ignoring the temporal term of the governing equation. The flow is introduced to the reactor by means of an external peristaltic or diaphragm pump operating at relatively low head of nearly 2-m to overcome the viscous shear stresses and head losses and the reactor vertical head at an adjustable discharge capacity of up to 5 L/min.

### 5.4. Simulation results

Based on the stoichiometry of transesterification reactive 3 moles of methanol are consumed with 1 mole of triglycerides for the making of 1 mole of biodiesel. Using this ratio(3:1 methanol to WCO molar), which also corresponds to AL/WCO mass fraction of 0.102/0.892, results on the species contour plots depicted in **Figure 8** and the outlet fractions are summarized in **Table 6**.

At this velocity and molar ration, a low conversion of 28% is achieved. The conversion is described by Eq. (16) and is written as:

$$Conv = \frac{C_{0,wco} - C_{f,wco}}{C_{0,wco}} \times 100 \tag{16}$$

where *C* is the concentration and the subscripts *o* and *f* signify the initial and final state of the concentration of the waste cooking oil (WCO). When the model is subjected to higher molar ratio of 6:1 AL to WCO and at higher inlet mass flow results are depicted in **Figure 9** of all the participating species. This figure illustrates the reaction takes place only within the inner tube ring. The conversion seems to be enhanced reaching as high as 89% based on the inlet and exit fraction evaluated in the inner loop of the tubular cylinder, however a considerable intermediate is still beside TG conversion and mandating the need for the flow to duel and additional residence time to complete the reaction.

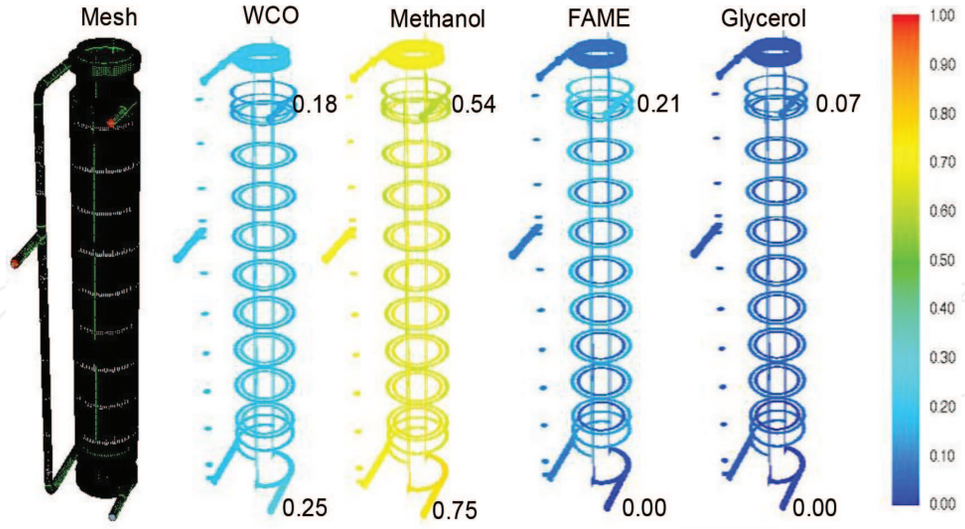


**Figure 8.** Molar fraction of species across the reactor (global scale).

| Port & ratio/species | $C_{54}H_{104}O_6$ (WCO) | $CH_4O$ | $C_{18}H_{36}O_2$ (FAME) | $C_3H_8O_3$ | Conversion |
|---|---|---|---|---|---|
| Inlet | 0.25 | 0.75 | 0 | 0 | 28% |
| Outlet | 0.18* | 0.54 | 0.21 | 0.07 | |

*Conversion = (0.25−0.18)/0.25.

**Table 6.** Species molar fraction at idealistic conditions.

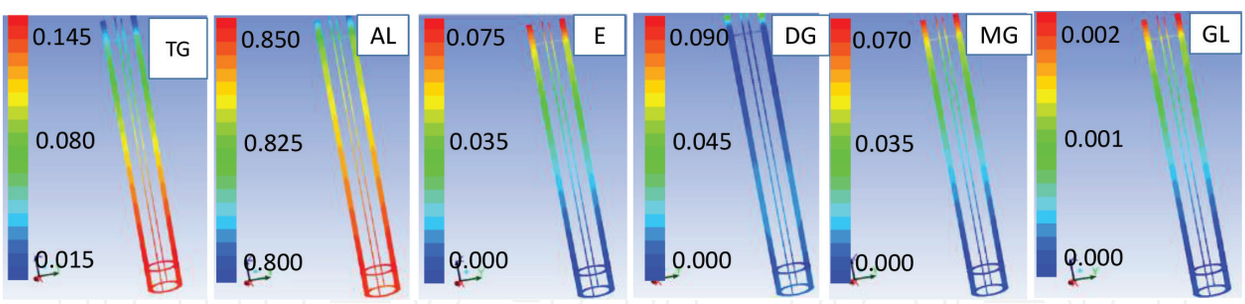


**Figure 9.** Molar fraction of the participating species within the first inner tube of the reactor and at 6:1 AL to WCO ratio.

From **Figure 9**, the concentration of the TG is reduced as the flow climbs up in the reactor as does the AL due to the production of biodiesel (E) and the two-intermediate species (MG and DG). The figure also clearly shows how DG precedes the formation of the MG and GL observed in the fading blue color contours of the DG concentration near the bottom inlet. The MG and GL show progressive color contours from the nil value represented by dark blue contours and reaching to higher value of 0.07 and 0.02 for each of MG and GL, respectively. Therefore, this allows additional residence time for the reaction in the second reactor tube reduces these intermediates and lead to higher production of the biodiesel and its byproduct

| Port & ratio/Species | $C_{54}H_{106}O_6$ (WCO) | $CH_4O$ | $C_{18}H_{36}O_2$ (FAME) | $C_3H_8O_3$ | Conversion |
|---|---|---|---|---|---|
| 3:1 methanol-WCO molar ratio | | | | | |
| Inlet | 0.25 | 0.75 | 0 | 0 | 0.66 |
| Outlet | 0.085 | 0.254 | 0.496 | 0.165 | |
| 6:1 methanol-WCO molar ratio | | | | | |
| Inlet | 0.143 | 0.857 | 0 | 0 | 0.66 |
| Outlet | 0.049 | 0.574 | 0.283 | 0.094 | |
| 9:1 methanol-WCO molar ratio | | | | | |
| Inlet | 0.10 | 0.90 | 0 | 0 | 0.66 |
| Outlet | 0.034 | 0.702 | 0.198 | 0.066 | |

**Table 7.** Species molar fraction at practical conditions.

glycerol. It must also be noted that these reactions are reversible and hence they can go either way, such that high conversion in the 1st tubular loop may be counter reacted by the second tubular loop and marking lower conversion.

Nevertheless, several sensitivity studies considering AL/WCO ratio, temperature, speed or mass flux of the feedstock etc. can be conducted. Results of the species concentration subjected to higher methanol ratio and larger influx of the feedstock of 600 mL/min (Re = 6000) are listed in **Table 7**. This result clearly marked a reasonable conversion of 66% which is higher than those obtained at lower influx %. The conversion seems also insensitive for the additional amount of the methanol which sounds counterintuitive initially and defies the experimental observation; this trend may be explained by the used kinetics which are inherited from the experimental work obtained at one ratio. These obtained values failed to capture the influence of the increase of the concentration of specific reactant to steer the reaction forward. Therefore, this may suggest another testing procedure at another molar ratio in parallel, mimicking those obtained and shown in **Figure 4**. Though, results emphasize the advantage of increasing residence time and efficient mixing of the flow which reduces the additional methanol concentration.

## 6. Conclusions

Transesterification of WCO to biodiesel is presented in this work and experimental and numerical analysis to this green process is presented. Initially, the chemical kinetics for the reaction are evaluated to the multiple reactions of the transesterification and in both the forward and reversal pathways for these reactions. The obtained kinetics presented by the activation energy (E) and the reaction pre-constant are evaluated and used to establish a high fidelity and robust reactive flow model. This model is based on computational fluid dynamics that is governed by the Navies-Stokes equations for isothermal, multiple species reactive flow

in turbulent regime. The model is built around the newly patented multiple tube and continuous transesterification reactor. The flow enters the reactor laterally and induces swirling flow. In turn, this results in an order of magnitude residence time higher than the transfer time that is based on the tube length and inlet velocity. Reactive flow at low velocity results in low conversion of the WCO, while actual turbulent flow significantly increases the conversion rate. Excess methanol mass sensitivity was insignificant to the conversion parameter that suggest that modeling can be still limited and suggesting to integrate more kinetics data. This work emphasizes the efficient mixing of the flow, interplaying as a parameter to the additional methanol concentration, thereby avoiding their downstream separation. In closing, numerical simulation of transesterification undoubtedly demonstrates the effectiveness of this tool in analyzing complicated reactive flow as the student faces in transesterification. Still, the process fails to reach completion even at higher reactant concentration and beyond the process stoichiometry. This creates an opportunity in this area to go beyond the conventional methods, such as electrical stimulation or signification and to assess their needed kinetics accordingly. The results demonstrate the feasibility of reactive flow dynamics in capturing and numerically simulating the transesterification process. This work substantiates the practicability of using numerical methods to construct precise and insightful image of the distribution of reaction rates and associated species to design and develop more efficient reactors.

## Acknowledgements

Khalifa University of Science and Technology, Masdar Institute Campus is highly acknowledged for their support.

## Author details

Isam Janajreh[1]* and Manar Almazrouei[2]

*Address all correspondence to: isam.janajreh@ku.ac.ae

1 Khalifa University of Science and Technology, Masdar City, Abu Dhabi, United Arab Emirates

2 Mechanical Engineering - (COE), United Arab Emirates University, Al Ain, UAE

## References

[1] Pradhan A, Shrestha DS. Impact of some common impurities on biodiesel cloud point. In: 2007 ASAE Annual Meeting. American Society of Agricultural and Biological Engineers; 2007. p. 1

[2] Banga S, Varshney PK. Effect of impurities on performance of biodiesel: A review. Journal of Scientific and Industrial Research. 2010;**69**(8):575-579

[3] Li Z, Ramanathan S, Chen C-C. Predicting thermophysical properties of mono-and diglycerides with the chemical constituent fragment approach. Industrial & Engineering Chemistry Research. 2010;**49**(11):5479-5484

[4] Ceriani R, Goncalves CB, Coutinho JAP. Prediction of viscosities of fatty compounds and biodiesel by group contribution. Energy & Fuels. 2011;**25**(8):3712-3717

[5] Noureddini H, Zhu D. Kinetics of transesterification of soybean oil. Journal of the American Oil Chemists' Society. 1997;**74**(11):1457-1463

[6] Janajreh I, ElSamad T, AlJaberi A, Diouri M. Transesterification of waste cooking oil: Kinetic study and reactive flow analysis. Energy Procedia. 2015;**75**:547-553

[7] Janajreh I, Al Shrah M. Numerical simulation of multiple step transesterification of waste oil in tubular reactor. Journal of Infrastructure Systems. 2016;**22**(4):A4014007

[8] Janajreh I, Almusharekh M, Ghenai C. Transesterification process of waste cooking oil: Catalyst synthesis, kinetic study, and modeling sensitivity. In: International Conference on Sustainable Solid Waste Management. 2014

[9] Janajreh I, ElSamad T. Mohammed Noorul Hussain, intensification of transesterification via sonication numerical simulation and sensitivity study. Applied Energy. 2017;**185**:2151-2159

[10] Janajreh I, Al Musharrekh M, Hussain M. Numerical simulation of transesterification and sensitivity study. International Journal of Modern Engineering. 2015;**15**(2):13-22

[11] Laidler KJ. The development of the Arrhenius equation. Journal of Chemical Education. 1984;**61**(6):494

[12] Abd Rabu R, Janajreh I, Honnery D. Transesterification of waste cooking oil: Process optimization and conversion rate evaluation. Energy Conversion and Management. 2013;**65**:764-769

[13] MATLAB. version 8.3.0 (R2014a). Natick, Massachusetts: The Math Works Inc.; 2014

[14] Freedman B, Butterfield RO, Pryde EH. Transeterfication kinetics of soybean oil. Journal of the American Oil Chemists' Society. 1986;**63**:1375-1380

[15] Freedman B, Pryde EH, Mounts TL. Variables affecting the yield of fatty esters from transesterfified vegetable oils. IBID. 1984;**61**:1638-1643

[16] Farkas L, Schachter O, Vromen BH. On the rate of acetate. Journal of the American Chemical Society. 1949;**71**:1991-1994

[17] Dufeck EJ, Butterfield RO, Frankel EN. Esterification and transsesterification of 9(10)-caboxystearic acid and its methyl esters, kinetic studies. Journal of the American Oil Chemists' Society. 1972;**49**:302-306

[18] Ansys Fluent 17.1. ANSYS Inc. Products; 2013

[19] Janajreh IM, Rabu RA. System and method for continuous transesterification of oils, US Patent 9,468,899; 2016

[20] Laidler K. The development of the Arrhenius equation. Journal of Chemical Education. 1984;**61**(6):494

[21] Narvaez PC, Rincon SM, Castaneda LZ, Sanchez FJ. Determination of some physical and transport properties of palm oil and of its methyl esters. Latin American Applied Research. 2008;**38**:1-6

[22] Cokljat D, Slack M, Vasquez SA. Reynolds-stress model for Eulerian multiphase. In: Hanjalic YNK, Tummers MJ, editors. Proceedings of the 4th International Symposium on Turbulence Heat and Mass Transfer. Begell House, Inc.; 2003. pp. 1047-1054

[23] Hinze JO. Turbulence. New York: McGraw-Hill Publishing Co.; 1975

[24] Fox RO. Computational Models for Turbulent Reacting Flows. Cambridge, England: Cambridge University Press; 2003